Different reactor configurations for enhancement of CO_2 methanation

Eleana Harkou[1], Sanaa Hafeez[2], Panayiota Adamou[1], Zhien Zhang[3] Anastasios I. Tsiotsias[4], Nikolaos D. Charisiou[3], Maria A. Goula [3], Sultan M. Al-Salem[5], George Manos [6], Achilleas Constantinou[1*]

[1]Department of Chemical Engineering, Cyprus University of Technology, 57 Corner of Athinon and Anexartisias, Limassol 3036, Cyprus;
[2]School of Engineering and Materials Science, Queen Mary University of London, London, E14NS, UK;
[3]WilliamG. Lowrie Department of Chemical and Biomolecular Engineerig, The Ohio State University Columbus, OH, 43210 USA
[4]Laboratory of Alternative Fuels and Environmental Catalysis (LAFEC), Department of Chemical Engineering, University of Western Macedonia, GR-50100, Greece;
[5]Environmental & Life Sciences Research Centre, Kuwait Institute for Scientific Research, Kuwait;
[6]Department of Chemical Engineering, University College London, London, WCIE7JE, UK.

*Corresponding author: Assist. Prof. Achilleas Constantinou (a.konstantinou@cut.ac.cy)

Abstract

Greenhouse gas emissions are a massive concern for scientists to minimize the effect of global warming in the environment. In this study, packed bed, coated wall, and membrane reactors were investigated using three novel nickel catalysts for the methanation of CO_2. CFD modelling methodologies were implemented to develop 2D models. The validity of the model was investigated in a previous study where experimental and simulated results in a packed bed reactor were in a good agreement. It was observed that the coated wall reactor had poorer performance compared to the packed bed, approximately 30 % difference between the results, as the residence time of the former was lower. In addition, two membrane configurations were proposed, including a membrane packed bed and membrane coated wall reactor. Additional studies were performed in the coated wall reactor revealing that lower flow rates lead to higher conversion values. As for the bed thickness the optimum layer was found to be 1 mm. In both membrane reactor configurations, the effect of the thickness of M_1 membrane, which indicates the membrane for the removal of H_2O, didn't show difference while the reduction of the thickness of M_2 membrane, which indicates the membrane for the removal of CO_2, H_2 and H_2O, showed better results in terms of conversion.

Keywords

CO_2 methanation; packed bed reactor; coated wall reactor; membrane reactor; CFD modelling.

1. Introduction

The global mean temperature increase is required to stabilized to 1.5 – 2 ^{o}C relative to the preindustrial era. In order to achieve that, the global yearly emissions must be net-zero or net-negative before 2100 [1,2]. The link between the carbon emissions with the globalization, economic growth and consumption of coal is positive with significant co-movements [3]. Carbon capture and utilization (CCU) technologies have attracted the interest of many scientists [4,5] as they can achieve reductions in CO_2 emissions along with sustainable energy technologies and technologies with negative or zero emissions [2]. It is important to reduce the cost and improve the performance of this technology in order to be utilized in large scales [6]. The generation of an energy carrier, CH_4, is creating a power-to-gas platform and a circular carbon economy [7–9]. The power-to-gas technology can be involved and contribute in the intermittent power production from renewable energy sources (RES) [10]. The firsts who proposed the CO_2 conversion to CH_4 were Sabatier and Senderens in 1902 [11] and it is described as [12]:

$$CO_2 + 4H_2 \leftrightarrow CH_4 + 2H_2O \quad (1)$$

The side-reactions that occur in parallel are the reverse water-gas shift (RWGS) and the CO methanation reactions and are involved in the methanation reaction, described by Eq. 2 and Eq. 3, respectively [12].

$$CO_2 + H_2 \leftrightarrow CO + H_2O \quad (2)$$

$$CO + 3H_2 \leftrightarrow CH_4 + H_2O \quad (3)$$

The utilization of CH_4 in industries is promising as it will reduce their energy demands and CO_2 emissions [13]. A plethora of studies have investigated different types of catalyst particles in an effort to optimize and enhance the conversion and selectivity of CO_2 methanation reaction over the time [14–22]. It is noted that these studies have been mostly carried out in packed bed reactors [23–26]. We note an earlier work from our group [27], in which we reviewed the CO_2 hydrogenation to valuable chemicals, including the CH_4 generation pathway, according to the challenges faced and the limitations between the convectional units and microreactors.

Coated wall reactors constitute a development of packed bed reactors where the solid catalyst particles are loaded and packed in a layer attached to the wall of the reactor. Coated

wall reactors provide lower pressure drops over the length of reactors cause of the form of drag, ease of the manufacturing [28], and faster heat exchange with the wall due to their intimate contact. Also, the approach of coated wall reactor would have been better for faster and more exothermic reactions rather than a traditional fixed bed reactor in order to obtain isothermal conditions. The gradients of radial concentrations might be considered as a potential drawback of coated wall reactors gradients by dispersion [29]. Danaci et al. [30], examined in a packed bed reactor 3D-structured catalysts prepared by depositioning fiber and coated with Ni/Al_2O_3 suspension, and compared them with powder Ni/Al_2O_3. The 3D-structured catalysts showed improvements in conversion and catalytic stability at higher temperatures. Huynh et al. [31], recently investigated bimetallic NiFe catalysts prepared. Temperature profiles along the reactor were derived from experimental results and computational fluid dynamics (CFD) studies. The packed bed configuration that was used in the study (low-high activity monolithic bed) achieved approximately 80% CH_4 yield at 250 ^oC. Moreover, Gruber et al. [32], optimized a coated wall reactor for CO_2 methanation. Both the 1D and 3D reactor models developed revealed the importance of external heat transfer. Adjustment in the layer of the catalyst by increasing its thickness revealed that the release of heat from the layer is increased while the heat transfer is reduced. Generally, the majority of studies use packed bed reactors during their investigations due to their economic efficiency. However, the coated wall reactor design for the CO_2 methanation reaction still lacks information, even though it can help optimize heat transfer and eliminate the pressure drop along the reactors.

Membrane reactors are a continuously developed technology with many advantages as they can operate the separation of various components and reactions in one system [33] reducing significantly the cost of a process. Moreover, reaction's yield can be improved as the selective separation of species can shift the equilibrium of a reaction. The Le Chatelier's principle is applied in order to restore the equilibrium [7]. Ohya et al. [34], used a membrane reactor in order to selectively remove the H_2O. Results revealed that the improvement in conversion was about 18% when a membrane reactor was used. Iwakiri et al. [35], used a non isothermal membrane reactor for the methanation of CO_2. The studied reactor and a fixed-bed reactor were compared using MATLAB; showing that the membrane reactor can achieve the same results, but at milder conditions. Another CFD study including the production of CH_4 using a heat-exchange membrane reactor was performed by Farisabadi et al. [36] and under optimal conditions a 99% CO_2 conversion was achieved.

The presence of CO_2 at industrial scale processes may cause corrosion or increase the volume of the gas transported in the pipelines, so the removal of CO_2 is a desired process. There are a lot of membrane types such as, polymeric, inorganic, metal-organic framework, zeolite and mixed-matrix membranes (MMMs) [37]. MMMs are combining the benefits of two types of membranes, the polymeric and inorganic, for the CO_2 removal from different gas fluids [38]. Wang et al. [39], investigated the separation CO_2/CH_4 using ZIF-301 filler in polyimide MMM revealing that the filler tended to improve the CO_2/CH_4 selectivity and the CO_2 permeability. Widiastuti et al. [40], aimed to enhance the CO_2 and H_2 removal efficiency from CH_4 with PSF/ZTC MMM. They showed the temperature effect and the TMOS concentration on membrane's performance by the reduction of pore size.

In this work, we carried out a theoretical investigation of different reactor designs, i.e., coated wall and membrane reactor configurations and compared their performance to a previous work published by our group for packed bed reactor [41]. Main goal was to assess their performance during CO_2 methanation and improve the conversion and selectivity of the reaction. CFD modelling studies offer better understanding of parameter optimization for different reactor systems [27], [42–49].

2. Modelling Methodology

A packed bed reactor was used for the experimental investigation of novel nickel catalysts on Pr-CeO_2 support synthesized using three different preparation methods. The catalyst's mass was 0.24 g and the space velocity was 25,000 ml g_{cat}^{-1} h^{-1}, while the reaction temperature varied between 200 and 450 ^{o}C. A theoretical investigation based on the experimental results was performed revealing the validation of the designed model. The full specifics of the previous experimental and theoretical work can be found in our previous work [41].

The theoretical investigation is an alternative solution to the experimental work as it requires less effort and expense. CFD models can determine the transport phenomena of heterogeneous flows within a reactor as well as important information of space-time variations in species flows, concentrations, and temperatures. Thus, CFD is a beneficial tool to predict parameters and to perform investigation of the physicochemical processes involved.

The reactor configurations presented by Figure 1 were designed as 2D configurations assuming that the gradients of concentrations and temperatures take place only in the radial and axial directions. Table 1 shows the geometrical properties of the reactor configurations that

were used in this work. Plug flow type is the overall flow transport mechanism that is operating in the axial direction. Additional assumptions that were incorporated in the model design are: (a) the solution of the study was stationary and temperature distribution was isothermally over the reactor, (c) all the gases behaved as ideal gases, (d) the transport coefficients and physical properties of the constant axial fluid velocity were uniform, and (e) the catalytic material in the reaction zone is in the form of powder. The investigation of internal and external limitations from the mass transfer resistance was occurred at a previous published work of our team. Experimentally and theoretically, the limitations of pressure drop, and heat transfer were found negligible. The reactor's height and length are 0.9 cm and 30 cm, respectively. The membrane materials that were used for the separation of gases are ZSM-5 and PDMS [50–52]. The membrane materials that were used in this work where: (i) the ZSM-5 membrane is selective to remove only H_2O; and (ii) the PDMS membrane is selective to remove CO_2, H_2 and H_2O from the gas mixture. The catalysts used herein are Ni-based supported catalysts, whose Pr-doped CeO_2 supports were prepared through different synthesis methods, i.e., citrate sol-gel synthesis (CSG), Pechini synthesis (PC) and modified Pechini synthesis (MPC). The Ni phase (10 wt%) was subsequently introduced into the prepared supports via wet impregnation and, as such, the corresponding catalysts were labelled as Ni/CSG, Ni/PC and Ni/MPC.

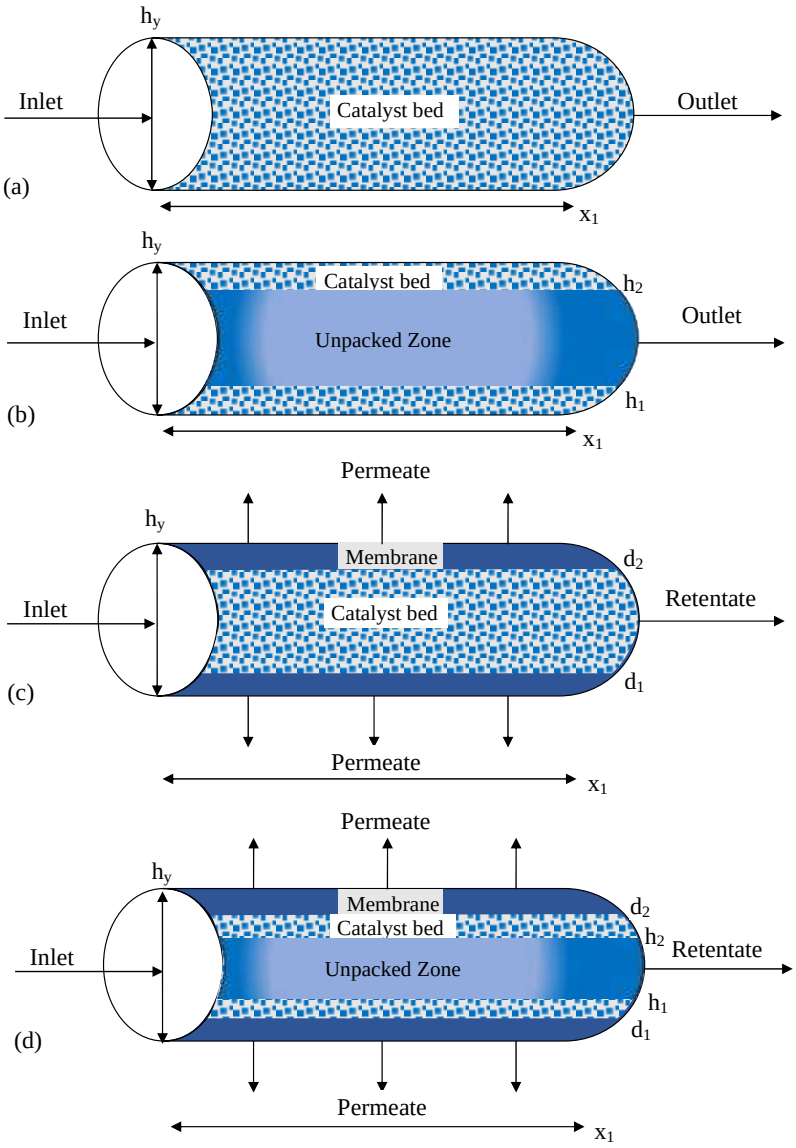

143

144 **Figure 1.** Reactor configurations designed for the CFD modelling study: (a) packed bed, (b)
145 coated wall, (c) membrane packed bed, and (d) membrane coated wall reactors.

146 **Table 1.** Geometrical properties of the reactor configurations.

Item	Value
Length of reactor (x_1)	30 cm
Packed bed reactor diameter (h_y)	0.9 cm
Each catalyst layer thickness	0.1 cm
Unpacked zone thickness (h_1,h_2)	0.7 cm
Each membrane layer thickness (d_1,d_2)	7 mm

147

2.1 Reaction rates

The kinetic model of CO_2 methanation reaction was firstly proposed by Xu and Froment [53], considering all three reactions for the methanation process (Eqs 1-3). The three reactions occur in parallel with the RWGS reaction converting CO_2 to CO, which thereafter generates CH_4 through the CO methanation reaction. The rate equations that describe the methanation reaction are given below (Eqs 4-6):

$$r_{CO2\ Meth.} = \frac{\frac{k_{CO_2\ Meth.}}{p_{H_2}^{3.5}}\left(p_{H_2}^4 p_{CO_2} - \frac{p_{CH_2} p_{H_2O}^2}{K_{eq,CO_2\ Meth.}}\right)}{\left(1 + K_{CO}p_{CO} + K_{H_2}p_{H_2} + K_{CH_4}p_{CH_4} + \frac{K_{H_2O}p_{H_2O}}{p_{H_2}}\right)^2} \quad (4)$$

$$r_{RWGS} = \frac{\frac{k_{RWGS}}{p_{H_2}}\left(p_{H_2} p_{CO_2} - \frac{p_{CO} p_{H_2O}}{K_{eq,RWGS}}\right)}{\left(1 + K_{CO}p_{CO} + K_{H_2}p_{H_2} + K_{CH_4}p_{CH_4} + \frac{K_{H_2O}p_{H_2O}}{p_{H_2}}\right)^2} \quad (5)$$

$$r_{CO\ Meth.} = \frac{\frac{k_{CO\ Meth.}}{p_{H_2}^{2.5}}\left(p_{H_2}^3 p_{CO_2} - \frac{p_{CO} p_{H_2O}}{K_{eq,CO\ Meth.}}\right)}{\left(1 + K_{CO}p_{CO} + K_{H_2}p_{H_2} + K_{CH_4}p_{CH_4} + \frac{K_{H_2O}p_{H_2O}}{p_{H_2}}\right)^2} \quad (6)$$

where $k_{CO_2\ Meth.}$, k_{RWGS}, $k_{CO\ Meth.}$ are the rate constants of reactions. K_{CO}, K_{H_2}, K_{CH_4} and, K_{H_2O} are the adsorption equilibrium constants and p_{CO_2}, p_{CO}, p_{H_2}, p_{CH_4} and p_{H_2O} are the partial pressure of species. By the constants Xu and Froment proposed in their model, the data according to kinetic and adsorption constants that were used for this CFD simulations were adjusted using parametric studies and can be found in a previous study [41]. There has been commodiously discussion in literature about the reaction intermediate of the methanation reaction with disagreement between different studies [54]. The three-step model used in this study is a Langmuir-Hinshelwood kinetic validated and used by many researchers [55–57] while it can address the CO_2 methanation and provide good agreement between experimental and simulated results [58].

2.2 Conservation equations

To design the reactor configurations mass balance equations were implicated for the transportation of species in the reactor. The Chemistry interface and the interface of Transport of Diluted Species with the feature of Reactive Pellet Bed are the physics that were employed

for this work using COMSOL Multiphysics. Eq. 7 describes the mass balance of species in the packed bed.

$$u_x \frac{\delta c_i}{\delta x} = D_{i,A} \frac{\delta^2 c_i}{\delta x^2} + D_{i,T} \frac{\delta^2 c_i}{\delta y^2} - J_i S_b \tag{7}$$

where, D_i and J_i are the coefficient of axial dispersion in the transverse or axial directions, and the fluid's molar flux in the powdered catalyst, respectively. The S_b is the catalyst's surface-active specific area in contact with the fluid reactants and is described as [59]:

$$S_b = \frac{3}{r_{pe}}(1 - \varepsilon) \tag{8}$$

where, ε is catalyst's bed void fraction and r_{pe} is the size of catalyst powder.

At the interface of pellet-fluid the film condition's assumption is made. The rate determined step can be the mass flux is related with mass balance and considered as boundary condition. The coefficient of external mass transfer is considered as the resistance and is described as:

$$J_i = h_i\left(c_i - c_{i,ps}\right) \tag{9}$$

$$h_i = \frac{Sh \cdot D_i}{2r_{pe}} \tag{10}$$

$$Sc = \frac{\mu}{\rho \cdot D_i} \tag{11}$$

$$Re = \frac{2r_p \cdot \rho \cdot u_x}{\mu} \tag{12}$$

$$Sh = 2 + 0.552 Re^{1/2} Sc^{1/3} \tag{13}$$

where, h_i and $c_{i,ps}$ are the coefficient of external mass transfer and species concentration at catalyst's surface. Sc, ρ and μ are the Schmidt number, the density, and the viscosity of the reacting fluids, respectively. Re is the Reynolds number and Sh is the Sherwood number [60,61].

The species mass balance equation in the unpacked area of coated wall reactor can be expressed as:

$$u_x \frac{\delta c_i}{\delta x} = D_i \left(\frac{\delta^2 c_i}{\delta x^2} + \frac{\delta^2 c_i}{\delta y^2} \right) \tag{14}$$

184 The reaction is occurring in the bed area where it is packed with catalyst in the form of
185 powder. Across the spherical shell mass balance of the powdered particle and an extra 1D
186 predefined dimension on the normalized radius ($r = r_{dim}/r_{pe}$) is expressed as:

$$4\pi N \left\{ r^2 r_{pe}^2 \varepsilon_{pe} \frac{\partial c_{pe,i}}{\partial t} + \nabla \cdot \left(-r^2 D_{i,eff} \nabla c_{pe,i} \right) = r^2 r_{pe}^2 R_{pe} \right\} \tag{15}$$

187 where, N is particles number, $D_{i,eff}$ is the effective diffusion coefficient of fluids in the pores
188 of powdered particle, $c_{pe,i}$ is the concentration of components in the powdered catalyst and R_{pe}
189 is the term of reaction rate.

190 Knudsen or bulk diffusion coefficients are considered to calculate the component species
191 effective diffusivities in the pores of the powdered catalysts expressed as [60]:

$$D_{i,eff} = \frac{D_{i,AB} \Phi_p \sigma_c}{\tau} \tag{16}$$

192 where, $D_{i,AB}$ is the diffusivity of fluid components in bulk, Φ_p is the porosity of the powdered
193 catalyst and σ_c and τ are the constriction factor and tortuosity, respectively.

194 The conservation equation of component species i transportation in the membrane is
195 described as:

$$D_{i,m} \left(\frac{\delta^2 c_{i,m}}{\delta x^2} + \frac{\delta^2 c_{i,m}}{\delta y^2} \right) = 0 \tag{17}$$

196 where, $c_{i,m}$ and $D_{i,m}$are the concentration and the species coefficient of diffusion, in the
197 membrane.

198 The Particle Tracing Module is a tool offered by COMSOL to find the distribution of
199 residence time by computing the direction of particles. The residence time distribution is
200 determined by the following equation where is an alternative to the first order Newtonian
201 formulation.

$$\frac{dq}{dt} = v \tag{18}$$

where, q is the pellet position (m) and v the velocity of the particle (m/s).

The boundary conditions used for investigated reactor configurations are given per following:

Coated-wall reactor:

$$\text{at } x = 0;\ c_i = c_{i,in} \tag{19}$$

$$\text{at } x = x_i;\ \frac{\delta c_i}{\delta x} = 0 \tag{20}$$

$$\text{at y} = 0;\ c_i = 0 \tag{21}$$

$$\text{at } r = 1;\ c_{i,p} = c_{i,ps} \tag{22}$$

$$\text{at } r = 0;\ \frac{\delta c_{i,p}}{\delta r} = 0 \tag{23}$$

$$\text{at } y = h_1;\ c_{i,b} = K \times c_i \tag{24}$$

$$\text{at } y = h_2;\ c_{i,b} = K \times c_i \tag{25}$$

Membrane packed bed reactor:

$$\text{at } x = 0;\ c_i = c_{i,in} \tag{26}$$

$$\text{at } x = x_i;\ \frac{\delta c_i}{\delta x} = 0 \tag{27}$$

$$\text{at y} = 0;\ c_i = 0 \tag{28}$$

$$\text{at } r = 1;\ c_{i,p} = c_{i,ps} \tag{29}$$

$$\text{at } r = 0;\ \frac{\delta c_{i,p}}{\delta r} = 0 \tag{30}$$

$$\text{at } y = d_1,\ y = d_2;\ c_{i,m} = Hc_i \tag{31}$$

$$\text{at } y = 0,\ y = h_y;\ c_{i,m} = c_{i,g} \tag{32}$$

Membrane coated-wall reactor:

$$\text{at } x = 0;\ c_i = c_{i,in} \tag{33}$$

$$\text{at } x = x_i;\ \frac{\delta c_i}{\delta x} = 0 \tag{34}$$

$$\text{at y} = 0;\ c_i = 0 \tag{35}$$

$$\text{at } r = 1;\ c_{i,p} = c_{i,ps} \tag{36}$$

$$\text{at } r = 0;\ \frac{\delta c_{i,p}}{\delta r} = 0 \tag{37}$$

$$\text{at } y = h_1;\ c_{i,b} = K \times c_i \tag{38}$$

$$\text{at } y = h_2;\ c_{i,b} = K \times c_i \tag{39}$$

$$\text{at } y = d_1,\ y = d_2;\ c_{i,m} = Hc_i \tag{40}$$

$$\text{at } y = 0,\ y = h_y;\ c_{i,m} = c_{i,g} \tag{41}$$

The software that was used for this work was the COMSOL Multiphysics in version 5.5 to couple all the boundary conditions, mass balances and conservation equations. Coated wall reactor's geometry had a mesh with domain elements of 2700 and degrees of freedom of 81270. The membrane packed bed microreactor model geometry had a mesh with domain elements of 2700 and degrees of freedom of 180600. The membrane coated wall microreactor model geometry had a mesh with domain elements of 2700 and degrees of freedom of 81270. The results for all the CFD models were found to be not influenced by the mesh as the solution was checked for higher degrees of freedom. The parameters used in this modelling study that were obtained from the experimental results are included in our previous published work [41].

3. Results and Discussion

3.1 Coated wall and membrane reactor

The results obtained from the CFD modelling studies are shown in this section. The validation of the model was examined in our previous study in packed bed reactor, where good agreement was observed from experimental and simulated results [41]. Coated wall and membrane reactors were investigated and compared to our previous work concerning the packed bed reactor. The reactors were operated at 1 atm and from 200 to 450 ^{o}C. The packed bed and coated wall reactor comparison is presented in Figure 2. It is observed from Figure 2(a), that the conversion of CO_2 in the coated wall reactor has decreased comparing to the performance of packed bed, and that can be attributed to the flow distribution inside the reactor.

In coated wall reactor the inner diameter is decreased, whilst the gas fluid velocity withing the reactor has increased for the same inlet flow rate. The mass of the catalyst used in both configurations was the same. Also, using the Particle Tracing Module offered by COMSOL, an investigation of the residence time of each reactor has occurred as there is no pressure drop or any mass and heat limitations to attribute the decrease of conversion in coated wall reactor. Residence time of the coated wall reactor was found to be 6.927 sec, and the residence time of the packed bed one was found to be around 11.451 sec, which is approximately 2 times than that of the coated wall reactor (Figure 2(c) and (d)). E(t) function is a fraction of molecules exiting the reactor that have spent a time t in the reactor. According to the residence time, we can assume that not all of the reactant molecules are passing through the thin catalyst layer of coated wall reactor, as the bed porosity is decreased. The selectivity was calculated considering the concentrations of CH_4 and CO with the equation given as $C_{CH4}/(C_{CH4} + C_{CO})$. The CH_4 selectivity (Figure 2(b)), decreases as the temperature increases, while the results between both reactors are similar. From this study it was obtained that the selectivity isn't influenced by the configurations of the coating layer since the amount of the catalyst used in packed bed and coated wall configurations is the same. The selectivity of a catalyst is mostly affected by the reaction conditions and the nature of the catalyst [62].

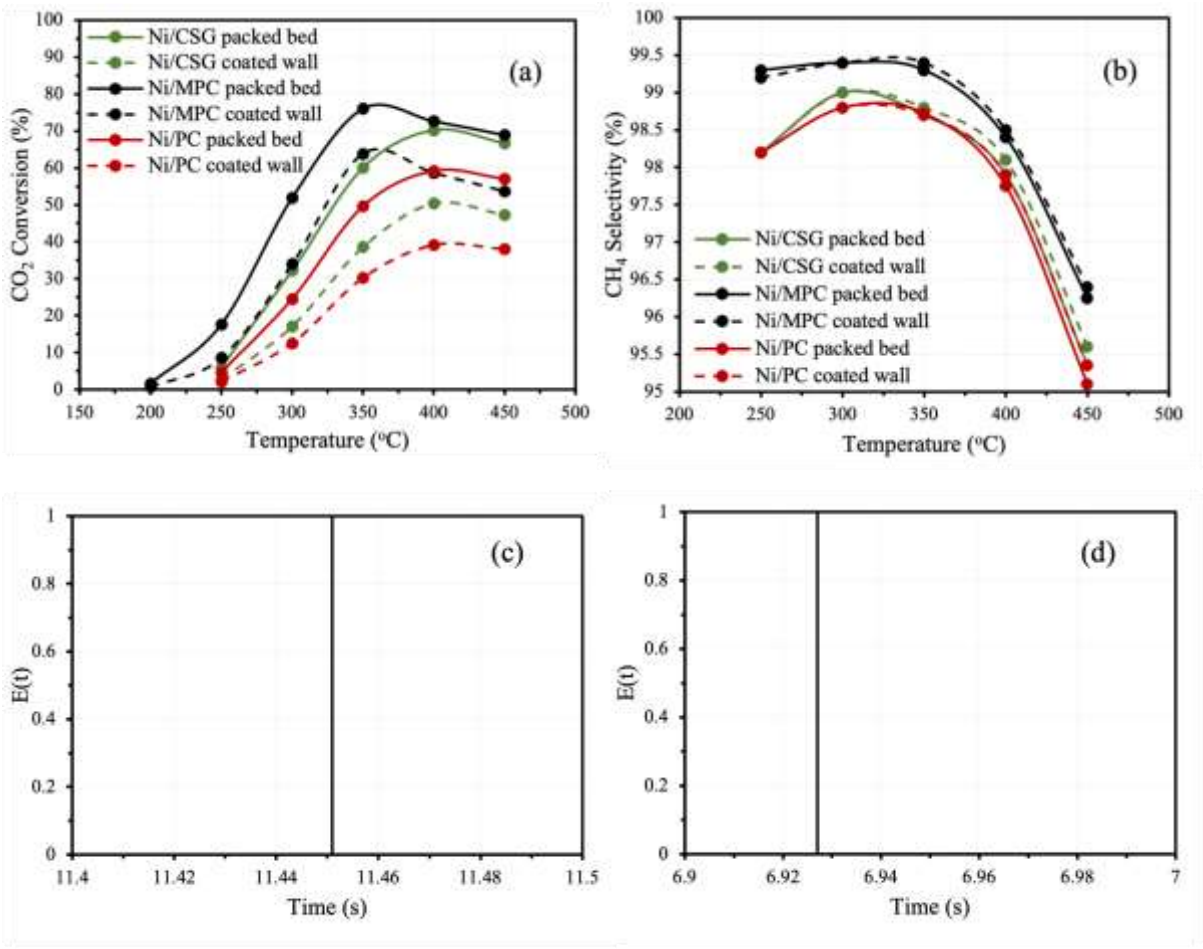

Figure 2. (a) CO_2 Conversion and (b) CH_4 Selectivity as a function of reactor temperature for the packed bed and the coated wall reactor. Residence Time Distribution in (c) the packed bed and (d) the coated wall reactor. Reaction conditions: WHSV = 25,000 ml g_{cat}^{-1} h^{-1}, bed porosity of packed bed 0.65 and bed porosity of coated wall 0.115.

The membrane modelling studies occurred for the best in performance catalyst, which is the Ni/MPC catalyst. M_1 and M_2 are the membrane configurations that were used in the CFD simulations. Membrane M_1 is selectively removing only H_2O and membrane M_2 is selectively separating CO_2, H_2 and H_2O from the gas mixture. By including the membranes in the reactor system, the methanation of CO_2 and the separation of various components is operating at the same time. The obtained results from both configuration studies can be found in Figure 3. It is observed from Figure 3(a), the conversion has slightly increased in packed bed reactor by using M_1 at higher temperatures. For the coated wall reactor, there is no significant difference between the initial study or with the addition of M_1. In both cases, almost 100% removal of H_2O is achieved. Removing the H_2O shifts the equilibrium of the reaction based on Le Chatelier's principle where is applied to restore the equilibrium and hence the CO_2 conversion

is increased. The scope of using the M_1 for the separation of H_2O only aims to increase the CO_2 conversion. Catarina Faria et al. [63], used a traditional packed bed reactor and a H-SOD membrane reactor with the simulated results revealing that the H_2O permeable membrane improved the CO_2 conversion and herein the performance of the reactor. The water permeable membrane Ohya et al. [34], revealed that the conversion was increased by a maximum of 18% with the membrane. A second membrane, M_2, was then investigated for the removal of CO_2, H_2 and H_2O. In packed bed reactor, it was observed from the figure that there is a slightly increase in the conversion, which it can be attributed to Le Chatelier's principle, while in coated wall reactor, no significant changes in the CO_2 conversion were observed. M_2 membrane not only removes H_2O, which is a product, but also the reactants. With the M_2 membrane, we aimed to create a single system where both reaction and separation of CH_4 from the other components can be achieved. CH_4 selectivity, as can be seen from Figure 3(b), remains constant in both reactors. The selectivity of the reaction is not influenced by the reactor configurations or the introduction of membranes in the system since the catalyst and the amount of the catalyst used for the computation studies was constant. Goswami et al. [64], compared three reactor configurations with the examined packed bed membrane, coated wall, and coated wall membrane reactors having a similar trend with our findings. The conversion in packed bed membrane reactor was obtained to be the optimum while the membrane coated wall reactor had better performance than the coated wall reactor.

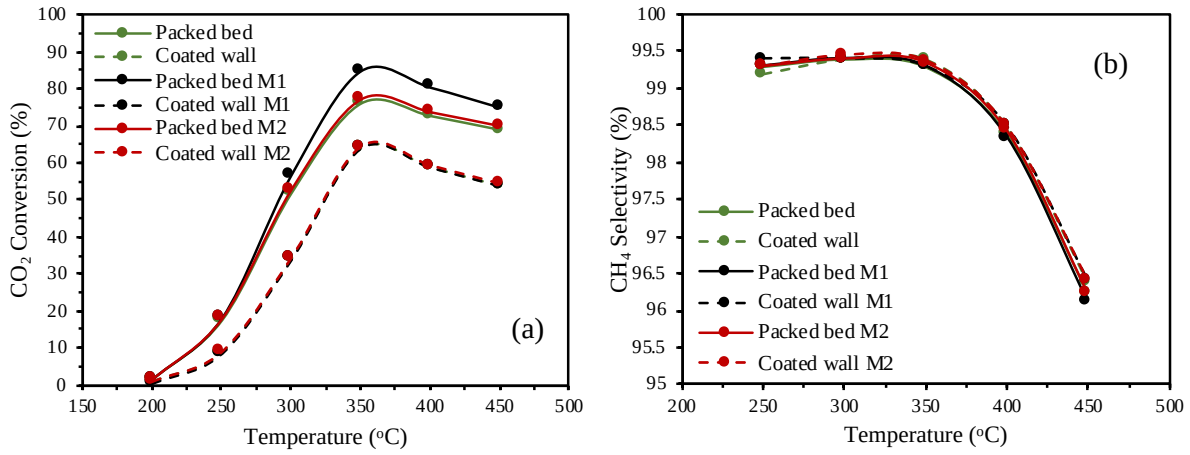

Figure 3. (a) CO_2 Conversion and (b) CH_4 Selectivity as a function of reactor temperature for the Ni/MPC catalyst in packed bed, coated wall, and membrane reactor configurations. Reaction conditions: WHSV = 25,000 ml g_{cat}^{-1} h^{-1}, bed porosity of packed bed 0.65 and bed porosity of coated wall 0.115.

3.2 Effect of flow rate in coated wall reactor

The conversion and selectivity were investigated how they're affected by the flow rate in this section in the coated wall reactor using the Ni/MPC catalyst. The initial inlet flow rate of the experimental and simulated studies was 100 ml/min. To enhance the methanation reaction in the coated wall reactor, a case study, was performed to examine the conversion of CO_2 at different inlet flow rates has occurred. 75, 50 and 25 ml/min flow rates were examined, and the results can be found in Figure 4. At lower inlet flow rates, the CO_2 conversion obtained higher values (Figure 4(a)). By decreasing the reactor's inlet flow rate, the fluid's velocity is also decreased and therefore the residence time of the fluid is affected. However, larger residence times led to increase of the conversion. The conversion and selectivity at 350 ^oC and 25 ml/min flow rate stand above 95 % and 99.3 %, respectively. Moreover, no significant differences in the selectivity of CH_4 are observed from Figure 4(b). Oh et al. [65], showed in a coated wall reactor, that the CH_4 conversion into olefins and higher hydrocarbons was affected by the flow rate having similar conversion trend as the one found in this study. At higher temperature and lower inlet flow rate, maximum conversion was achieved.

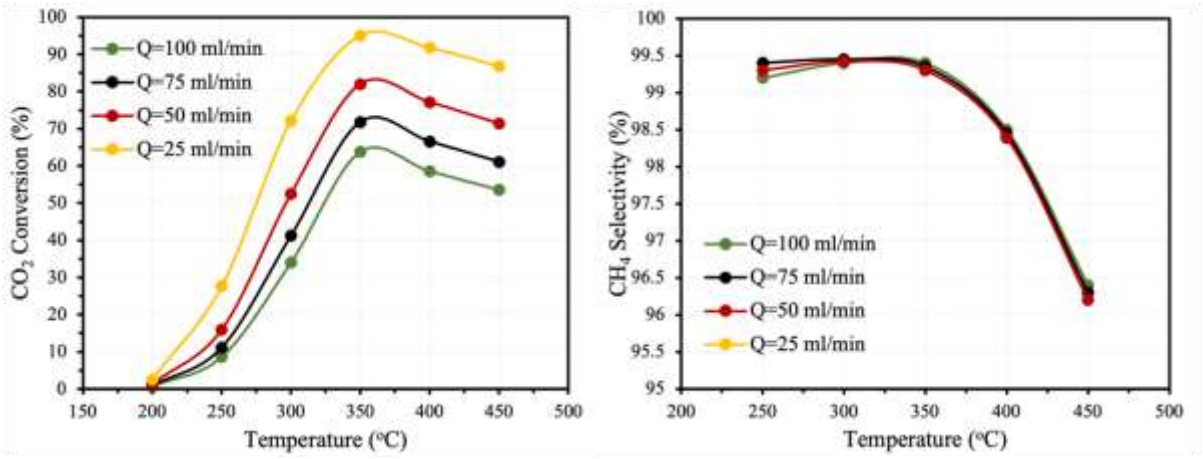

Figure 4. (a) CO_2 Conversion and (b) CH_4 Selectivity as a function of reactor temperature for the Ni/MPC catalyst in coated wall reactor at different flow rates. Reaction conditions: Bed porosity of coated wall 0.115.

3.3 Effect of bed thickness in coated wall reactor

In the initial study of coated wall, the bed thickness of each layer was 1 mm. The bed thickness is important and contributes to the conversion of CO_2. The thickness is related with the bed porosity, the reactor's inner diameter and herein fluid's flow rate and velocity. In this section, a comprehensive case study was held combining all these parameters that are affected

by the thickness of the catalyst bed for the best performing catalyst (Ni/MPC), and the results are presented in Figure 5. Four, different in thickness, coating layers were investigated, 0.9, 1, 1.5 and 2 mm for each layer, with bed porosities of 0.027, 0.115, 0.37 and 0.494, respectively, at 350 ^{o}C and catalyst mass of 0.24 g. By reducing the flow rates, it is obtained an improvement in the conversion due to fluid's larger residence time. Moreover, the less thicker the catalyst layer, the higher the conversion. It's also observed that there is an optimum coating layer where the conversion attains a maximum value. By decreasing the thickness of the catalyst bed further, at 0.9 mm, a decrease in conversion was observed when compared to that of the coating layer with 1 mm thickness. This can be attributed to the respective porosities, where in the first case the porosity is very small obstructing the smooth transport of components in the coating area. As can be observed, the coated wall reactor with 1 mm catalyst coating has the optimum layer, with bed porosity of 0.115 and 20 ml/min flow rate reaching 97% conversion of CO_2.

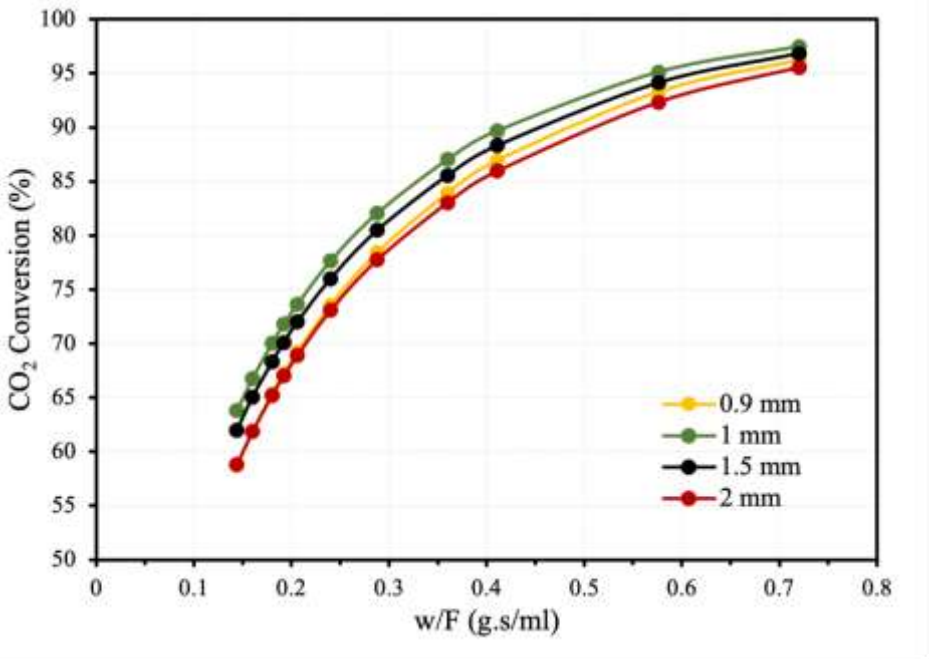

Figure 5. CO_2 Conversion as a function of the weight of catalyst/volumetric flow rate for the Ni/MPC catalyst in coated wall reactor at 350 ^{o}C. Thickness of coating layers 0.9, 1, 1.5 and 2 mm each and bed porosities of 0.027, 0.115, 0.37 and 0.494, respectively, are presented.

3.4 Effect of membrane thickness in packed bed and coated wall reactors

The effect of the thickness of the membrane on conversion of CO_2 and selectivity for CH_4 is discussed in this section. The initial membrane modeling study that occurred, investigated two membranes, M_1 and M_2, where both had the same thickness of 7 mm. The thickness of the membrane is related with its permeability and herein affects the removal efficiency of the

components. In this study, three membrane thickness values were investigated, 7, 1, and 0.1 mm, for the best performing catalyst Ni/MPC, and with all the other parameters remaining constant. The M_1 membrane didn't show any difference in the results in both configurations (not shown). This might be attributed to the fact that at 7 mm membrane thickness 100 % removal of H_2O was already achieved, and that further reduction of membrane thickness didn't show any difference in the results. In contrast, at the initial study of the M_2 membrane, the CO_2, H_2 and H_2O removal was not 100 %. Figure 6 shows the conversion and selectivity of CO_2 and for CH_4, respectively, for the M_2 membrane. By decreasing the thickness of membrane, the mass transfer coefficient in membrane and flux of the separated components are increased, which led to better separation. In addition, Le' Chatelier's principle is implemented to restore the equilibrium and the conversion of CO_2 is increased (Figure 6(a)). As for the selectivity for CH_4, it can be observed from Figure 6(b) that no significant differences were obtained. Figure 6 (c) shows the conversion of CO_2 for both M_2 membrane configurations as a function of membrane thickness. Decreasing the membrane thickness from 7 to 1 mm did not significantly change the conversion while the conversion increase was more obvious for membrane thickness between 0.1 – 1 mm. By decreasing the membrane thickness, the permeability of species is tended to increase with more species being removed from the reactor and higher conversions of CO_2 are obtained according to Le' Chatelier's principle. Packed bed M_2 membrane reactor with 0.1 mm membrane thickness, bed porosity of 0.65 and 100 ml/min flow rate, had the best performance, with CO_2 conversion of over 98 % with CH_4 selectivity of 99.4 %. The thickness of membranes should be kept minimal within manufacturing possibilities in order to achieve the maximum separation of components and reduce the manufacturing cost.

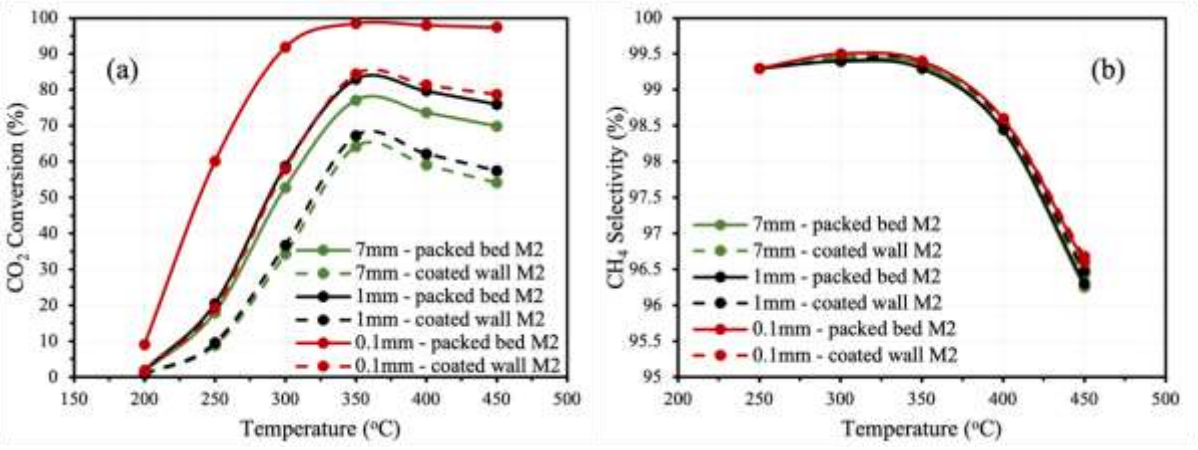

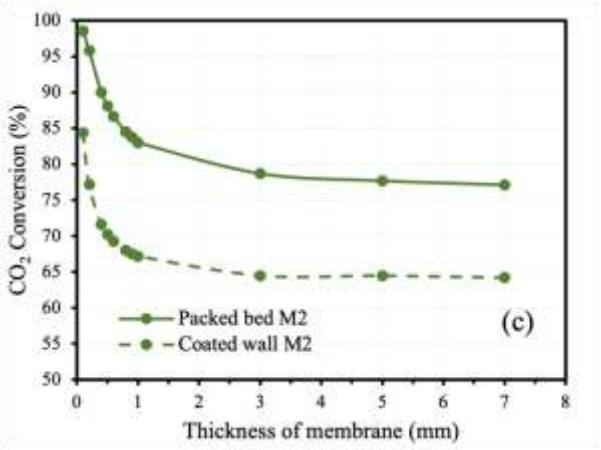

353

354 **Figure 6.** (a) CO_2 Conversion and (b) CH_4 Selectivity as a function of reactor temperature for
355 the Ni/MPC catalyst in M_2 packed bed and M_2 coated wall membrane reactors at different
356 membrane thickness. (c) CO_2 Conversion as a function of membrane thickness for the Ni/MPC
357 catalyst in M_2 packed bed and M_2 coated wall at 350 ^oC. Reaction conditions: WHSV = 25,000
358 ml g_{cat}^{-1} h^{-1}, bed porosity of packed bed 0.65 and bed porosity of coated wall 0.115.

359 ## 4. Conclusions

360 In this work, four different reactor configurations were investigated and compared based
361 on their CO_2 methanation catalytic performance. The packed bed reactor, which was initially
362 investigated in our previous study, displayed a higher CO_2 conversion than the coated wall
363 reactor, as the residence time of packed bed was higher. Therefore, two different membranes,
364 M_1 and M_2, which were able to separate solely H_2O (M_1) and CO_2, H_2 and H_2O (M_2), were
365 included in the modelling. The packed bed membrane reactor showed that the separation of the
366 reaction components tended to increase the CO_2 conversion, while the coated wall membrane
367 reactor didn't show any significant difference in results. Additional case studies in the coated
368 wall reactor of the flow rate effect on the CO_2 conversion showed that at lower flow rates,
369 higher CO_2 conversion values are achieved. Moreover, the investigation of the bed thickness
370 in the coated wall reactor revealed that the optimum layer of the catalyst coating was 1 mm
371 with bed porosity of 0.115 and flow rate of 20 ml/min, where 97% CO_2 conversion was
372 reached. As for the membrane thickness in both membrane reactor configurations, it was shown
373 that there was no impact on CO_2 conversion for the M_1 membrane, while for the M_2 membrane,
374 its reduction improved the CO_2 conversion. It was revealed that the packed bed M_2 membrane
375 reactor with 0.1 mm membrane thickness, bed porosity of 0.65 and 100 ml/min flow rate had
376 the best performance, reaching CO_2 conversion of over 98 % and CH_4 selectivity of 99.4 %.

The study of 3D CFD models regarding the CO_2 methanation reaction using all the same simulation constants and parameters that were used in this study will be performed in a future work as well as the examination of the veritableness of the performance of each reactor. Moreover, the comparison between different kinetic rates for the CO_2 methanation reaction will be performed to obtain substantial results. These fundamental findings may help develop new or improve already existing reactor configurations to further enhance the methanation reaction's performance.

References

[1] J. DeAngelo *et al.*, "Energy systems in scenarios at net-zero CO2 emissions," *Nature Communications*, vol. 12, no. 1, p. 6096, Oct. 2021, doi: 10.1038/s41467-021-26356-y.

[2] H. Mikulčić *et al.*, "Flexible Carbon Capture and Utilization technologies in future energy systems and the utilization pathways of captured CO2," *Renewable and Sustainable Energy Reviews*, vol. 114, p. 109338, 2019.

[3] C. Huo *et al.*, "Recent scenario and nexus of globalization to CO2 emissions: Evidence from wavelet and Quantile on Quantile Regression approach," *Environmental Research*, vol. 212, p. 113067, Sep. 2022, doi: 10.1016/j.envres.2022.113067.

[4] W. Gao *et al.*, "Industrial carbon dioxide capture and utilization: state of the art and future challenges," *Chem. Soc. Rev.*, vol. 49, no. 23, pp. 8584–8686, 2020, doi: 10.1039/D0CS00025F.

[5] C. Yuan, Z. Pan, Y. Wang, F. M. Baena-Moreno, A. Constantinou, and Z. Zhang, "Carbon Capture Enhancement by Water-Based Nanofluids in a Hollow Fiber Membrane Contactor," *Energy Technology*, vol. n/a, no. n/a, p. 2300254, Apr. 2023, doi: 10.1002/ente.202300254.

[6] W. J. Lee *et al.*, "Recent trend in thermal catalytic low temperature CO2 methanation: A critical review," *Catalysis Today*, vol. 368, pp. 2–19, 2021.

[7] J. Ashok, S. Pati, P. Hongmanorom, Z. Tianxi, C. Junmei, and S. Kawi, "A review of recent catalyst advances in CO2 methanation processes," *Catalysis Today*, vol. 356, pp. 471–489, 2020.

[8] A. I. Tsiotsias, N. D. Charisiou, I. V. Yentekakis, and M. A. Goula, "Bimetallic ni-based catalysts for CO2 methanation: A review," *Nanomaterials*, vol. 11, no. 1, p. 28, 2020.

[9] A. I. Tsiotsias, N. D. Charisiou, I. V. Yentekakis, and M. A. Goula, "The role of alkali and alkaline earth metals in the CO2 methanation reaction and the combined capture and methanation of CO2," *Catalysts*, vol. 10, no. 7, p. 812, 2020.

[10] C. H. Tan, S. Nomanbhay, A. H. Shamsuddin, Y.-K. Park, H. Hernández-Cocoletzi, and P. L. Show, "Current Developments in Catalytic Methanation of Carbon Dioxide—A Review," *Frontiers in Energy Research*, vol. 9, p. 795423, 2022.

[11] P. Sabatier and J. Senderens, "Comptes Rendus Des Séances De L'Académie Des Sciences, Section VI–Chimie," *Paris: Imprimerie Gauthier-Villars*, 1902.

[12] C. Choi *et al.*, "Determination of Kinetic Parameters for CO2 Methanation (Sabatier Reaction) over Ni/ZrO2 at a Stoichiometric Feed-Gas Composition under Elevated Pressure," *Energy & Fuels*, vol. 35, no. 24, pp. 20216–20223, 2021, doi: 10.1021/acs.energyfuels.1c01534.

[13] M. C. Bacariza, D. Spataru, L. Karam, J. M. Lopes, and C. Henriques, "Promising Catalytic Systems for CO2 Hydrogenation into CH4: A Review of Recent Studies," *Processes*, vol. 8, no. 12, 2020, doi: 10.3390/pr8121646.
[14] S. Tada, T. Shimizu, H. Kameyama, T. Haneda, and R. Kikuchi, "Ni/CeO2 catalysts with high CO2 methanation activity and high CH4 selectivity at low temperatures," *International Journal of Hydrogen Energy*, vol. 37, no. 7, pp. 5527–5531, Apr. 2012, doi: 10.1016/j.ijhydene.2011.12.122.
[15] S. Tada, O. J. Ochieng, R. Kikuchi, T. Haneda, and H. Kameyama, "Promotion of CO2 methanation activity and CH4 selectivity at low temperatures over Ru/CeO2/Al2O3 catalysts," *International Journal of Hydrogen Energy*, vol. 39, no. 19, pp. 10090–10100, Jun. 2014, doi: 10.1016/j.ijhydene.2014.04.133.
[16] A. Makdee, P. Kidkhunthod, Y. Poo-arporn, and K. C. Chanapattharapol, "Enhanced CH4 selectivity for CO2 methanation over Ni-TiO2 by addition of Zr promoter," *Journal of Environmental Chemical Engineering*, vol. 10, no. 3, p. 107710, Jun. 2022, doi: 10.1016/j.jece.2022.107710.
[17] F. Liu, Y. S. Park, D. Diercks, P. Kazempoor, and C. Duan, "Enhanced CO2 Methanation Activity of Sm0.25Ce0.75O2-δ–Ni by Modulating the Chelating Agents-to-Metal Cation Ratio and Tuning Metal–Support Interactions," *ACS Appl. Mater. Interfaces*, vol. 14, no. 11, pp. 13295–13304, Mar. 2022, doi: 10.1021/acsami.1c23881.
[18] M. C. Bacariza, I. Graça, J. M. Lopes, and C. Henriques, "Enhanced activity of CO2 hydrogenation to CH4 over Ni based zeolites through the optimization of the Si/Al ratio," *Microporous and Mesoporous Materials*, vol. 267, pp. 9–19, Sep. 2018, doi: 10.1016/j.micromeso.2018.03.010.
[19] S. Kikkawa, K. Teramura, H. Asakura, S. Hosokawa, and T. Tanaka, "Isolated Platinum Atoms in Ni/γ-Al2O3 for Selective Hydrogenation of CO2 toward CH4," *J. Phys. Chem. C*, vol. 123, no. 38, pp. 23446–23454, Sep. 2019, doi: 10.1021/acs.jpcc.9b03432.
[20] G. I. Siakavelas *et al.*, "Highly selective and stable nickel catalysts supported on ceria promoted with Sm2O3, Pr2O3 and MgO for the CO2 methanation reaction," *Applied Catalysis B: Environmental*, vol. 282, p. 119562, 2021.
[21] G. I. Siakavelas *et al.*, "Highly selective and stable Ni/La-M (M= Sm, Pr, and Mg)-CeO2 catalysts for CO2 methanation," *Journal of CO2 Utilization*, vol. 51, p. 101618, 2021.
[22] A. I. Tsiotsias *et al.*, "Optimizing the oxide support composition in Pr-doped CeO2 towards highly active and selective Ni-based CO2 methanation catalysts," *Journal of Energy Chemistry*, vol. 71, pp. 547–561, 2022.
[23] M. M. Jaffar, M. A. Nahil, and P. T. Williams, "Parametric Study of CO2 Methanation for Synthetic Natural Gas Production," *Energy Technology*, vol. 7, no. 11, p. 1900795, Nov. 2019, doi: 10.1002/ente.201900795.
[24] A. Bengaouer, J. Ducamp, I. Champon, and R. Try, "Performance evaluation of fixed-bed, millistructured, and metallic foam reactor channels for CO2 methanation," *The Canadian Journal of Chemical Engineering*, vol. 96, no. 9, pp. 1937–1945, Sep. 2018, doi: 10.1002/cjce.23140.
[25] R. T. Zimmermann, J. Bremer, and K. Sundmacher, "Optimal catalyst particle design for flexible fixed-bed CO2 methanation reactors," *Chemical Engineering Journal*, vol. 387, p. 123704, May 2020, doi: 10.1016/j.cej.2019.123704.
[26] B. Kreitz, G. D. Wehinger, and T. Turek, "Dynamic simulation of the CO2 methanation in a micro-structured fixed-bed reactor," *Chemical Engineering Science*, vol. 195, pp. 541–552, Feb. 2019, doi: 10.1016/j.ces.2018.09.053.
[27] S. Hafeez *et al.*, "Hydrogenation of carbon dioxide (CO 2) to fuels in microreactors: a review of set-ups and value-added chemicals production," *Reaction Chemistry & Engineering*, 2022.

[28] J. Bravo, A. Karim, T. Conant, G. P. Lopez, and A. Datye, “Wall coating of a CuO/ZnO/Al2O3 methanol steam reforming catalyst for micro-channel reformers,” *Chemical Engineering Journal*, vol. 101, no. 1, pp. 113–121, Aug. 2004, doi: 10.1016/j.cej.2004.01.011.
[29] R. J. Berger and F. Kapteijn, “Coated-Wall Reactor ModelingCriteria for Neglecting Radial Concentration Gradients. 1. Empty Reactor Tubes,” *Ind. Eng. Chem. Res.*, vol. 46, no. 12, pp. 3863–3870, Jun. 2007, doi: 10.1021/ie0612313.
[30] S. Danaci, L. Protasova, J. Lefevere, L. Bedel, R. Guilet, and P. Marty, “Efficient CO2 methanation over Ni/Al2O3 coated structured catalysts,” *Catalysis Today*, vol. 273, pp. 234–243, Sep. 2016, doi: 10.1016/j.cattod.2016.04.019.
[31] H. L. Huynh, W. M. Tucho, Q. Shen, and Z. Yu, “Bed packing configuration and hot-spot utilization for low-temperature CO2 methanation on monolithic reactor,” *Chemical Engineering Journal*, vol. 428, p. 131106, Jan. 2022, doi: 10.1016/j.cej.2021.131106.
[32] M. Gruber *et al.*, “Modeling and Design of a Catalytic Wall Reactor for the Methanation of Carbon Dioxide,” *Chemie Ingenieur Technik*, vol. 90, no. 5, pp. 615–624, May 2018, doi: 10.1002/cite.201700160.
[33] Z. Wang, J. Ashok, Z. Pu, and S. Kawi, “Low temperature partial oxidation of methane via BaBi0.05Co0.8Nb0.15O3−δ-Ni phyllosilicate catalytic hollow fiber membrane reactor,” *Chemical Engineering Journal*, vol. 315, pp. 315–323, May 2017, doi: 10.1016/j.cej.2017.01.015.
[34] H. Ohya *et al.*, “Methanation of carbon dioxide by using membrane reactor integrated with water vapor permselective membrane and its analysis,” *Journal of Membrane Science*, vol. 131, no. 1, pp. 237–247, Aug. 1997, doi: 10.1016/S0376-7388(97)00055-0.
[35] I. G. I. Iwakiri, A. C. Faria, C. V. Miguel, and L. M. Madeira, “Split feed strategy for low-permselective membrane reactors: A simulation study for enhancing CO2 methanation,” *Chemical Engineering and Processing - Process Intensification*, vol. 163, p. 108360, Jun. 2021, doi: 10.1016/j.cep.2021.108360.
[36] A. FarisAbadi, M. Kazemeini, and A. Ekramipooya, “Investigating a HEX membrane reactor for CO2 methanation using a Ni/Al2O3 catalyst: A CFD study,” *International Journal of Hydrogen Energy*, Aug. 2022, doi: 10.1016/j.ijhydene.2022.06.290.
[37] M. Chawla *et al.*, “Membranes for CO2/CH4 and CO2/N2 gas separation,” *Chemical Engineering & Technology*, vol. 43, no. 2, pp. 184–199, 2020.
[38] N. Jusoh, Y. F. Yeong, T. L. Chew, K. K. Lau, and A. M. Shariff, “Current development and challenges of mixed matrix membranes for CO2/CH4 separation,” *Separation & Purification Reviews*, vol. 45, no. 4, pp. 321–344, 2016.
[39] Z. Wang *et al.*, “ZIF-301 MOF/6FDA-DAM polyimide mixed-matrix membranes for CO2/CH4 separation,” *Separation and Purification Technology*, vol. 264, p. 118431, 2021.
[40] N. Widiastuti *et al.*, “Annealing and TMOS coating on PSF/ZTC mixed matrix membrane for enhanced CO2/CH4 and H2/CH4 separation,” *Royal Society open science*, vol. 9, no. 6, p. 211371, 2022.
[41] A. I. Tsiotsias *et al.*, “Enhancing CO2 methanation over Ni catalysts supported on sol-gel derived Pr2O3-CeO2: An experimental and theoretical investigation,” *Applied Catalysis B: Environmental*, vol. 318, p. 121836, 2022.
[42] S. Hafeez, E. Aristodemou, G. Manos, S. M. Al-Salem, and A. Constantinou, “Computational fluid dynamics (CFD) and reaction modelling study of bio-oil catalytic hydrodeoxygenation in microreactors,” *React. Chem. Eng.*, vol. 5, no. 6, pp. 1083–1092, 2020, doi: 10.1039/D0RE00102C.
[43] S. Hafeez, E. Aristodemou, G. Manos, S. M. Al-Salem, and A. Constantinou, “Modelling of packed bed and coated wall microreactors for methanol steam reforming for hydrogen

production," *RSC Adv.*, vol. 10, no. 68, pp. 41680–41692, 2020, doi: 10.1039/D0RA06834A.
[44] S. Hafeez *et al.*, "Decomposition of Additive-Free Formic Acid Using a Pd/C Catalyst in Flow: Experimental and CFD Modelling Studies," *Catalysts*, vol. 11, no. 3, 2021, doi: 10.3390/catal11030341.
[45] S. Hafeez *et al.*, "Computational Investigation of Microreactor Configurations for Hydrogen Production from Formic Acid Decomposition Using a Pd/C Catalyst," *Ind. Eng. Chem. Res.*, vol. 61, no. 4, pp. 1655–1665, Feb. 2022, doi: 10.1021/acs.iecr.1c04128.
[46] S. Hafeez, S. M. Al-Salem, G. Manos, and A. Constantinou, "Fuel production using membrane reactors: a review," *Environmental Chemistry Letters*, vol. 18, no. 5, pp. 1477–1490, Sep. 2020, doi: 10.1007/s10311-020-01024-7.
[47] E. Harkou, S. Hafeez, G. Manos, and A. Constantinou, "CFD Study of the Numbering up of Membrane Microreactors for CO2 Capture," *Processes*, vol. 9, no. 9, 2021, doi: 10.3390/pr9091515.
[48] G. Wu, E. Cao, P. Ellis, A. Constantinou, S. Kuhn, and A. Gavriilidis, "Development of a flat membrane microchannel packed-bed reactor for scalable aerobic oxidation of benzyl alcohol in flow," *Chemical Engineering Journal*, vol. 377, p. 120086, Dec. 2019, doi: 10.1016/j.cej.2018.10.023.
[49] A. Constantinou, G. Wu, B. Venezia, P. Ellis, S. Kuhn, and A. Gavriilidis, "Aerobic Oxidation of Benzyl Alcohol in a Continuous Catalytic Membrane Reactor," *Topics in Catalysis*, vol. 62, no. 17, pp. 1126–1131, Nov. 2019, doi: 10.1007/s11244-018-1060-9.
[50] Z. Li *et al.*, "High Temperature Water Permeable Membrane Reactors for CO2 Utilization," *Chemical Engineering Journal*, vol. 420, p. 129834, Sep. 2021, doi: 10.1016/j.cej.2021.129834.
[51] H. Lin *et al.*, "Dehydration of natural gas using membranes. Part I: Composite membranes," *Journal of Membrane Science*, vol. 413–414, pp. 70–81, Sep. 2012, doi: 10.1016/j.memsci.2012.04.009.
[52] T. Merkel, V. Bondar, K. Nagai, B. Freeman, and I. Pinnau, "Gas sorption, diffusion, and permeation in poly (dimethylsiloxane)," *Journal of Polymer Science Part B: Polymer Physics*, vol. 38, no. 3, pp. 415–434, 2000.
[53] J. Xu and G. F. Froment, "Methane steam reforming, methanation and water-gas shift: I. Intrinsic kinetics," *AIChE J.*, vol. 35, no. 1, pp. 88–96, Jan. 1989, doi: 10.1002/aic.690350109.
[54] M. S. Duyar, A. Ramachandran, C. Wang, and R. J. Farrauto, "Kinetics of CO2 methanation over Ru/γ-Al2O3 and implications for renewable energy storage applications," *Journal of CO2 Utilization*, vol. 12, pp. 27–33, Dec. 2015, doi: 10.1016/j.jcou.2015.10.003.
[55] S. Renda, A. Ricca, and V. Palma, "Insights in the application of highly conductive structured catalysts to CO2 methanation: Computational study," *International Journal of Hydrogen Energy*, Feb. 2023, doi: 10.1016/j.ijhydene.2023.01.338.
[56] B. Hwang *et al.*, "Reaction Characteristics of Ni-Based Catalyst Supported by Al2O3 in a Fluidized Bed for CO2 Methanation," *Catalysts*, vol. 12, no. 11, 2022, doi: 10.3390/catal12111346.
[57] P. Costamagna, F. Pugliese, T. Cavattoni, G. Busca, and G. Garbarino, "Modeling of Laboratory Steam Methane Reforming and CO2 Methanation Reactors," *Energies*, vol. 13, no. 10, 2020, doi: 10.3390/en13102624.
[58] J. Zhang, N. Fatah, S. Capela, Y. Kara, O. Guerrini, and A. Y. Khodakov, "Kinetic investigation of carbon monoxide hydrogenation under realistic conditions of methanation of biomass derived syngas," *Fuel*, vol. 111, pp. 845–854, Sep. 2013, doi: 10.1016/j.fuel.2013.04.057.

[59] J. Richardson, J. Harker, and J. Backhurst, “Flow of fluids through granular beds and packed columns,” *Chemical engineering*, vol. 2, pp. 191–236, 2002.
[60] H. S. Fogler, *Elements of chemical reaction engineering*. Third edition. Upper Saddle River, N.J. : Prentice Hall PTR, [1999] ©1999, 1999. [Online]. Available: https://search.library.wisc.edu/catalog/999810177702121
[61] N. Froessling, “Über die verdunstung fallender tropfen,” *Gerlands Beiträge zur Geophysik*, vol. 52, no. 1, pp. 170–216, 1938.
[62] J. I. Gray and L. F. Russell, “Hydrogenation catalysts—Their effect on selectivity,” *Journal of the American Oil Chemists’ Society*, vol. 56, no. 1, pp. 36–44, Jan. 1979, doi: 10.1007/BF02671758.
[63] A. Catarina Faria, C. V. Miguel, A. E. Rodrigues, and L. M. Madeira, “Modeling and Simulation of a Steam-Selective Membrane Reactor for Enhanced CO2 Methanation,” *Ind. Eng. Chem. Res.*, vol. 59, no. 37, pp. 16170–16184, Sep. 2020, doi: 10.1021/acs.iecr.0c02860.
[64] N. Goswami, K. K. Singh, S. Kar, and R. C. Bindal, “Numerical simulations of HI decomposition in coated wall membrane reactor and comparison with packed bed configuration,” *Applied Mathematical Modelling*, vol. 40, no. 21, pp. 9001–9016, Nov. 2016, doi: 10.1016/j.apm.2016.05.051.
[65] S. C. Oh *et al.*, “Direct Non-Oxidative Methane Conversion in a Millisecond Catalytic Wall Reactor,” *Angewandte Chemie International Edition*, vol. 58, no. 21, pp. 7083–7086, May 2019, doi: 10.1002/anie.201903000.